nature neuroscience

Ucn3 and CRF-R2 in the medial amygdala regulate complex social dynamics

Yair Shemesh[1,2,5], Oren Forkosh[1,2,5], Mathias Mahn[1], Sergey Anpilov[1,2], Yehezkel Sztainberg[1], Sharon Manashirov[1,2], Tamar Shlapobersky[1,2], Evan Elliott[3], Laure Tabouy[3], Gili Ezra[1,2], Elaine S Adler[1,2], Yair J Ben-Efraim[1,2], Shosh Gil[1,2], Yael Kuperman[4], Sharon Haramati[1], Julien Dine[2], Matthias Eder[2], Jan M Deussing[2], Elad Schneidman[1], Ofer Yizhar[1] & Alon Chen[1,2]

Social encounters are associated with varying degrees of emotional arousal and stress. The mechanisms underlying adequate socioemotional balance are unknown. The medial amygdala (MeA) is a brain region associated with social behavior in mice. Corticotropin-releasing factor receptor type-2 (CRF-R2) and its specific ligand urocortin-3 (Ucn3), known components of the behavioral stress response system, are highly expressed in the MeA. Here we show that mice deficient in CRF-R2 or Ucn3 exhibit abnormally low preference for novel conspecifics. MeA-specific knockdown of *Crfr2* (*Crhr2*) in adulthood recapitulated this phenotype. In contrast, pharmacological activation of MeA CRF-R2 or optogenetic activation of MeA Ucn3 neurons increased preference for novel mice. Furthermore, chemogenetic inhibition of MeA Ucn3 neurons elicited pro-social behavior in freely behaving groups of mice without affecting their hierarchal structure. These findings collectively suggest that the MeA Ucn3–CRF-R2 system modulates the ability of mice to cope with social challenges.

In social environments, individual interests may be confronted with the needs and expectations of others[1]. Thus, the ability to respond adequately to social stimuli is important for facilitating adaptive social interactions. Such socioemotional skills reflect how individuals perceive themselves and others[2]. Because of the complexity of social environments, adequate coping with the stress that accompanies social engagements requires highly adaptive behavior. Such coping is compromised in a variety of psychiatric disorders, such as social anxiety disorder and autism spectrum disorders, which are both characterized by dysfunctional reciprocal social interactions and altered coping with the social environment[3,4]. Since the nature of social ties has a crucial effect on our physical health[5], even mild difficulties in coping with the social environment can be maladaptive. Understanding of the molecular mechanisms and neurobiological circuits that regulate the socioemotional balance is limited, and our ability to intervene and treat maladaptive social stress is poor.

The central corticotropin-releasing factor (CRF) system helps mediate the neuroendocrine and behavioral responses to stressful challenges[6]. CRF plays a well-established role in the regulation of the hypothalamic-pituitary-adrenal axis under basal and stress conditions and is proposed to integrate the autonomic, metabolic, and behavioral responses to stressors[6]. In addition to CRF, the mammalian CRF peptide family contains urocortins 1, 2 and 3 (Ucn1, Ucn2 and Ucn3), and their effects are mediated, with different affinities, through activation of two known receptors, CRF receptor types 1 and 2 (CRF-R1 and CRF-R2)[6]. Dysregulation of the CRF system has been linked to stress-related emotional disorders such as anxiety and depression[6].

Ucn3, the only highly selective ligand for CRF-R2, is expressed in distinct brain nuclei including the MeA, the bed nucleus of stria terminalis (BNST), the median preoptic nucleus, and the perifornical area of the hypothalamus[7,8]. CRF-R2 also displays distinct and restricted expression, being expressed in the MeA, the BNST, the ventromedial hypothalamic nucleus (VMH), the lateral septum (LS) and the dorsal raphe[9]. Interestingly, many of these regions overlap with the 'mammalian social brain network', which consists of the MeA, BNST, LS, median preoptic nucleus, VMH, midbrain, and anterior hypothalalmus[10]. This suggests that coping with the stress imposed by social interactions may rely on a mechanism that involves Ucn3 and CRF-R2.

The MeA, in which both CRF-R2 and Ucn3 are expressed, is a central hub in the rodent's social brain network. It is the first site where signals from the olfactory bulb and vomeronasal system converge, thus positioning the MeA to recognize, analyze, and categorize incoming chemosensory information[11]. This makes the MeA a critical center for processing pheromonal signals that regulate social behavior. Indeed, the MeA facilitates the ability of a mouse to discriminate between chemosignals of different conspecifics[12]. We hypothesized that manipulating the MeA Ucn3–CRF-R2 system would affect the way mice cope with the challenges of interacting with either novel or familiar conspecifics.

A considerable portion of our knowledge of social behavior in mice is based on dyadic paradigms of short duration, in which interactions are tested between a single pair of animals. These strictly controlled experiments are relatively easy to perform in the laboratory and have

[1]Department of Neurobiology, Weizmann Institute of Science, Rehovot, Israel. [2]Department of Stress Neurobiology and Neurogenetics, Max Planck Institute of Psychiatry, Munich, Germany. [3]Faculty of Medicine, Bar Ilan University, Safed, Israel. [4]Department of Veterinary Resources, Weizmann Institute of Science, Rehovot, Israel. [5]These authors contributed equally to this work. Correspondence should be addressed to A.C. (alon.chen@weizmann.ac.il).

Received 9 May; accepted 22 June; published online 18 July 2016; doi:10.1038/nn.4346

been highly fruitful and instructive in many studies[13,14]. However, in nature, mice form groups with complex and flexible social structures, depending on the habitat and availability of resources[15]. Thus, social phenotypes manifested outside of naturally relevant social contexts might be misinterpreted or indiscernible[16]. This notion has attracted increasing attention in recent years and led to the development of new behavioral models for tracking the behavior of groups of mice in a semi-natural context[17–19].

To investigate the role of the MeA Ucn3–CRF-R2 system in regulating social coping, we performed a series of experiments in which we used several molecular and neuronal manipulations: germline knockout (KO) of *Ucn3* or *Crfr2* genes, conditional knockdown (KD) of MeA *Crfr2* mRNA, pharmacological activation of MeA CRF-R2, and optogenetic activation of MeA Ucn3 neurons. Following each manipulation, we measured social behavior in a short dyadic test to establish the preference of mice for conspecifics (familiar and novel) or for a nonsocial area. We also chemogenetically inhibited MeA Ucn3 cells subchronically, for a period of 3 d, using DREADD-based technology and monitored the behavior of individual mice in a group over several days in a semi-natural environment. This multidisciplinary approach revealed the involvement of the MeA Ucn3–CRF-R2 system in mediating the ability to cope with the challenge of social engagement.

RESULTS

Germline *Ucn3* KO and *Crfr2* KO mice avoid novel conspecifics

To investigate the role of the Ucn3–CRF-R2 system in the regulation of social approach and avoidance, we used a dyadic test that is based on the social approach test (**Supplementary Fig. 1a**)[20]. In our modified version, we used automated means to quantify the tendency of a male 'actor' mouse to remain in a remote (nonsocial) chamber or to pursue interactions with two different conspecifics: a nest-mate sibling or a novel mouse. The actor was habituated to a dimly lit (1 lx) arena, composed of three connected chambers that were open from above, each the size of a standard home cage. By entering a certain chamber, the actor chose to investigate, through a mesh, either the littermate (a familiar male) or the unfamiliar male or else to stay in the nonsocial area. The gaps in the mesh enabled olfactory as well as limited tactile contact between the actor and the conspecifics. The test duration was 30 min. We found that *Crfr2* KO mice displayed stronger preference for familiar mice relative to wild-type (WT) controls (**Fig. 1a**) and that both *Crfr2* KO and *Ucn3* KO mice avoided novel conspecifics relative to the WT controls (**Fig. 1a**,**b**). By contrast, *Crfr2* KO and *Ucn3* KO mice were similar to WT mice in their nonsocial exploratory behavior (**Supplementary Fig. 1c**,**d**) and novelty-seeking behavior (**Fig. 1c**,**d** and **Supplementary Fig. 1b**), suggesting that this phenotype might be specifically social.

Mapping the MeA Ucn3–CRF-R2 circuit

We hypothesized that Ucn3 and CRF-R2 neurons in the MeA regulate socioemotional balance during interactions with conspecifics. Consequently, we expected that MeA Ucn3 and MeA CRF-R2 neurons would be connected to other regions of the mouse social brain network.

To visualize the MeA CRF-R2 cells, we used a mouse line expressing Cre recombinase under the control of the *Crfr2* promoter (*Crfr2::Cre*) and a reporter allele encoding the red fluorescent protein tdTomato upon Cre-mediated recombination (*Rosa26-CAG-lsl-tdtomato*, Ai9). Ai9 cellular expression in the brains of *Crfr2::Cre* mice closely matched that of *Crfr2* mRNA as described by Van Pett *et al.*[9], including the MeA (**Supplementary Fig. 2**). We confirmed the expression of *Crfr2* and *Ucn3* in the MeA that was previously outlined[7,9], using anti-Ucn3 immunostaining of brain slices from *Crfr2::Cre::Ai9* mice (**Fig. 2a**).

Next we studied the circuitry of these two neuronal populations using different tracing methods. To identify monosynaptic inputs to MeA Ucn3 cells, we used Cre-dependent trans-synaptic retrograde tracing[21] to bilaterally transduce MeA neurons of C57BL/6X129 mice expressing Cre recombinase under the control of the *Ucn3* promoter (*Ucn3::Cre* mice; see **Supplementary Fig. 3** for line validation). Mice were injected with conditional helpers (AAV5-EF1a-FLEX-TVA-mCherry and AAV8-CAG-FLEX-RG and a conditional rabies virus SADΔG-GFP(EnvA). This resulted in eYFP expression in MeA Ucn3$^+$ neurons, as well as in cells from regions known to project to the MeA (**Supplementary Fig. 4a**). Cells that were retrogradely labeled were present in three presynaptic regions[22,23]: the olfactory tubercle, the BNST, and the PVN (**Fig. 2b** and **Supplementary Fig. 4b**). The olfactory tubercle is an important center for encoding odor valence[24], the BNST is suggested to be a valence surveillance hub in the mouse social brain network[25] and the PVN is known to mediate social behavior through central and peripheral release of nonapeptides[26].

To identify synaptic outputs from the MeA Ucn3 cells, we again used the *Ucn3::Cre* mice, but with a virus-mediated Cre-recombinase-dependent anterograde transneuronal tracer based on the H129 strain of herpes simplex virus (H129 TK-TT)[27], which was delivered to MeA Ucn3 cells. In these mice, fluorescence identifies neurons that are

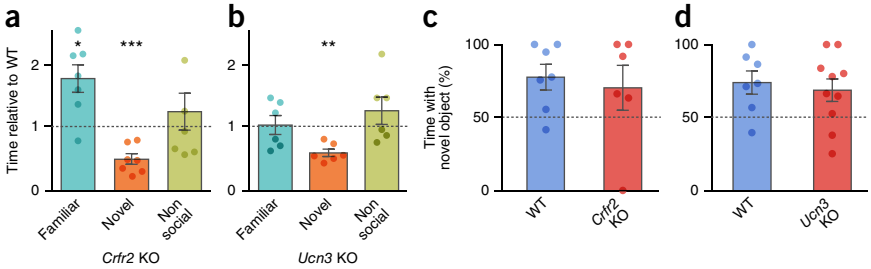

Figure 1 *Crfr2* and *Ucn3* deficient mice display altered social approach in the social maze test but normal novel object preference. (**a**) The time the *Crfr2* KO mice ($n = 7$) spent in each chamber relative to control WT littermates ($n = 8$). The *Crfr2* KO mice did not spend equal time to WT mice in each chamber (repeated-measures (RM) one-way ANOVA $P = 0.0145$, $F(2) = 6.151$), and thus they significantly differed from controls. The *Crfr2* KO mice spent significantly more time investigating the familiar mouse (two-tailed *t*-test, $P = 0.015$, $t = 2.801$, d.f. = 13) and less time investigating the novel mouse (two-tailed *t*-test, $P = 0.0005$, $t = 4.587$, d.f. = 13) compared to controls. (**b**) The time the *Ucn3* KO mice ($n = 6$) spent in each chamber relative to control WT littermates ($n = 7$). The *Ucn3* KO mice did not spend equal time to WT mice in each chamber (RM one-way ANOVA $P = 0.0362$, $F(2) = 5.545$), and thus they significantly differed from controls. The *Ucn3* KO mice did not differ from controls in time spent investigating the familiar mice (two-tailed *t*-test, $P = 0.9098$, $t = 0.116$, d.f. = 11) but did differ from controls in time investigating the novel mouse (two-tailed *t*-test, $P = 0.0076$, $t = 3.263$, d.f. = 11). (**c**) *Crfr2* KO mice did not differ from WT littermates in the novel object preference test (two-tailed Student's *t*-test ($n = 6$ and 7 respectively, $P = 0.6623$, $t = 0.4488$, d.f. = 11). (**d**) *Ucn3* KO mice did not differ from WT littermates in the novel object preference test (two-tailed Student's *t*-test, $n = 10$ and 7 respectively, $P = 0.6525$, $t = 0.4594$, d.f. = 15). Data are mean ± s.e.m. n is the number of animals, $^*P < 0.05$, $^{**}P < 0.01$, $^{***}P < 0.001$.

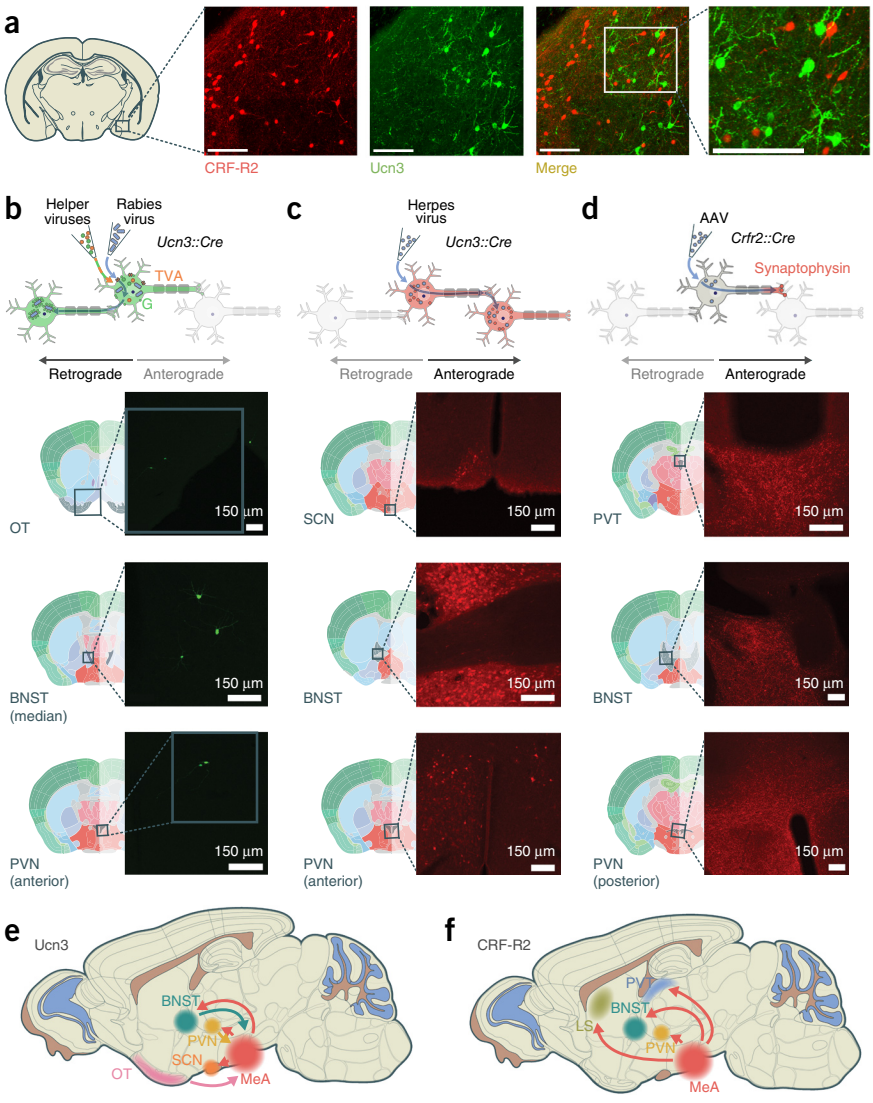

Figure 2 The MeA Ucn3–CRF-R2 circuit is embedded within the social brain network. (**a**) *Crfr2::Cre* mice carry a conditional tdTomato reporter, showing CRF-R2-expressing cells in the MeA (red). Ucn3 is detected by immunostaining (green). Scale bars represent 50 µm ($n = 3$ mice). (**b**) Monosynaptic inputs (green cells) to MeA Ucn3 neurons ($n = 2$ mice). OT, olfactory tubercle. (**c**) Synaptic outputs from MeA Ucn3 neurons. Red cells indicate the tdTomato marker expressed in cells anterograde to MeA *Ucn3::Cre*-expressing cells ($n = 3$ mice). (**d**) Efferent projections from MeA CRF-R2 cells. Red dots in top panel represent presynaptic puncta of MeA CRF-R2 projections ($n = 3$ mice). Top panels in **b**–**d** illustrate the viral tracing techniques. (**e**) Distribution of input and output projections to MeA Ucn3 neurons. (**f**) Distribution of output projections from MeA CRF-R2 neurons.

post-synaptic to the MeA Ucn3 cells (**Fig. 2c** and **Supplementary Fig. 4c**). We identified three regions that receive projections from the MeA Ucn3 neurons: the suprachiasmatic nucleus (SCN) (responsible for control of circadian rhythms), the BNST, and the PVN. All three regions are known to receive projections from the MeA[28].

To identify regions receiving projections from the MeA CRFR2 neurons, we injected a viral vector encoding a Cre-dependent mCherry reporter fused to synaptophysin into the MeA of *Crfr2::Cre* mice (AAV9-CMV-Flex-synaptophysin-mCherry)[29]. In these mice, red puncta indicate presynaptic boutons originating from MeA CRF-R2 expressing neurons. We identified four regions containing labeled presynaptic terminals: the paraventricular thalamic nucleus (PVT) the BNST, the PVN, and the LS (**Fig. 2d** and **Supplementary Fig. 4d**). The PVT is thought to modulate approach-avoidance behavior and defensive behavioral responses[30]. These findings demonstrate that, as expected, Ucn3 and CRF-R2 cells in the MeA both receive inputs from and project to limbic regions that are part of the mouse social brain network (**Fig. 2e**,**f**).

MeA *Crfr2* knockdown mice avoid novel conspecifics

To investigate the role of MeA Ucn3–CRF-R2 system in the regulation of social approach and avoidance, we used a lentiviral approach to knock down *Crfr2* specifically in the MeA or, as a control, the LS (**Fig. 3a**). A lentivirus encoding shRNA targeting the *Crfr2* transcript (sh*Crfr2*) was designed and verified as previously described[31]. Mice were tested using the dyadic social approach test, 10 d following a bilateral stereotaxic injection of either sh*Crfr2* or a control virus into the MeA of C57BL/6J naive mice. Like *Crfr2* KO mice, MeA *Crfr2* KD mice showed more interest in familiar mice and reduced interest in novel mice (**Fig. 3b**). By contrast, LS *Crfr2* KD mice did not differ from controls (**Fig. 3c**). We found no significant differences between MeA *Crfr2* KD and control mice in nonsocial anxiety-like behavior in the open field test, in the dark-light transfer test or in home-cage locomotor activity (**Fig. 3d**,**e** and **Supplementary Fig. 5a**–**d**).

mUcn3 delivery to MeA increases interest in novel conspecifics

Next we determined the physiological and behavioral effects of MeA CRF-R2 neuronal activation by application of mouse (m) Ucn3. We performed patch-clamp recordings in MeA slices from *Crfr2::Cre::Ai9* mice (**Fig. 4a**,**b**). CRF-R2-expressing neurons exhibited a voltage sag upon hyperpolarizing current injections and a rebound burst following cessation of the current injection (**Fig. 4c**) in 7 of 8 stably recorded cells (≥30 min). The combination of these electrophysiological properties is characteristic for a majority of MeA GABAergic cells, but it is not observed for non-GABAergic MeA neurons[32]. These findings are also corroborated by our *in situ* hybridization data, showing that in the MeA the majority of *Crfr2*-expressing cells coexpress GAD65 and 67 (*Gad2*/*Gad1*) (**Supplementary Fig. 6**). Under blockade of ionotropic glutamate and GABA receptors, bath application of mUcn3 (100 nM) caused a depolarization of the neurons (**Fig. 4c**,**d**). This effect was accompanied by an increase in the neuronal input resistance (**Fig. 4c**,**e**). Consistent with the resultant enhanced excitability, we further found that the neurons fired more action potentials (APs) in response to positive current injections following exposure to mUcn3 (**Fig. 4c**,**f**).

Next, using the social approach test, we studied the behavioral effect of mUcn3 delivery to the MeA. We surgically cannulated naive

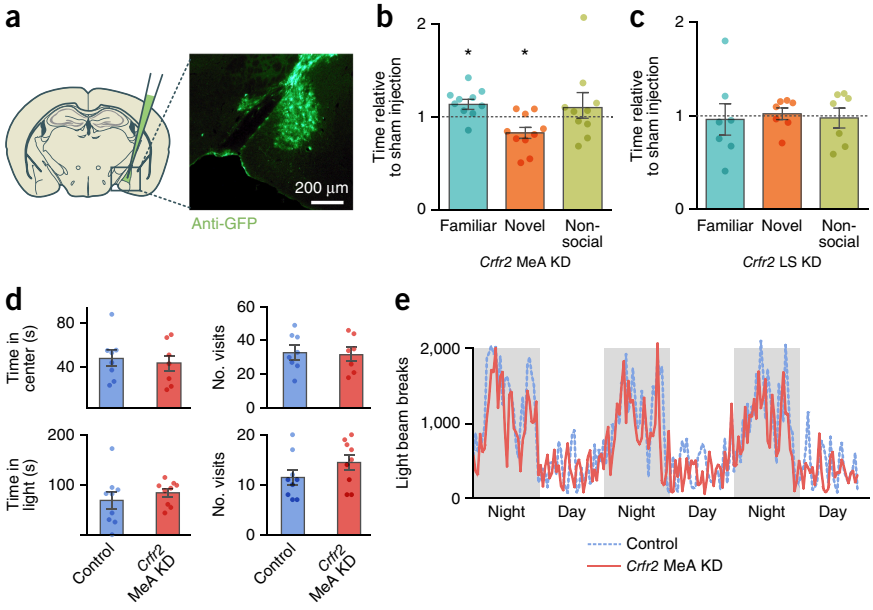

Figure 3 MeA *Crfr2* KD mice show higher preference for novel conspecifics. (**a**) GFP immunostaining showing the specific delivery of sh*Crfr2* KD lentiviral vector to the MeA of adult male mice ($n = 10$ sham-injected controls and 10 KD mice). (**b**) Time spent by MeA *Crfr2* KD mice ($n = 10$) in each chamber, relative to control sham-injected mice ($n = 10$). The MeA *Crfr2* KD mice (RM one-way ANOVA $P = 0.0359$, $F(2) = 4.026$). The MeA *Crfr2* KD mice spent significantly more time investigating the familiar mice (one-tailed *t*-test, $P = 0.033$, $t = 1.957$, d.f. = 18) and less time investigating differed from controls in the amount of time spent in each chamber the novel mice (one-tailed *t*-test, $P = 0.0441$, $t = 1.803$, d.f. = 18) compared to controls. (**c**) The time spent by LS *Crfr2* KD mice ($n = 7$) in each chamber, relative to control LS sham-injected mice ($n = 5$). The LS *Crfr2* KD mice did not differ from LS sham-injected control in time spent in each chamber (RM one-way ANOVA $P = 0.8836$, $F(2) = 0.045$). (**d**) MeA *Crfr2* KD mice did not display any changes in anxiety-like behavior compared to controls ($n = 7$ controls and 8 KD), as revealed by the open field test (time in center: two-tailed *t*-test, $P = 0.656$, $t = 0.454$, d.f. = 13; number of visits: two-tailed *t*-test, $P = 0.844$, $t = 0.199$, d.f. = 13) and the light/dark transfer test ($n = 9$ controls and 9 KD; time in light: two-tailed *t*-test, $P = 0.601$, $t = 0.533$, d.f. = 16; number of visits: two-tailed *t*-test, $P = 0.176$, $t = 0.1413$, d.f. = 16). (**e**) General locomotor activity, as measured during 3 consecutive days, revealed no differences in the total activity between control mice ($n = 10$) and *Crfr2*-R2 MeA KD mice ($n = 10$) during the light and dark phases of the day (RM two-way ANOVA, $P = 0.1689$, $F(1) = 2.055$). Data are mean ± s.e.m. *n* is the number of animals, $^*P < 0.05$.

C57BL/6J mice. Following a 2-week recovery period, mice were injected with mUcn3 peptide (treatment) or artificial cerebrospinal fluid (aCSF; control) directly into the MeA and tested 20 min later in the social approach test. Activation of MeA CRF-R2 resulted in an opposite behavioral phenotype from KD of the receptor in the MeA. Mice treated with mUcn3 spent more time near novel mice and less time near familiar mice, as compared to controls (**Fig. 4g**). As expected, this phenotype disappeared when treatment was preceded with MeA injection of Astressin 2B, a CRF-R2-specific antagonist (**Fig. 4h**; controls received aCSF and mUcn3 before treatment). Treated mice were similar to control mice in their nonsocial exploratory behavior (**Supplementary Fig. 7a–d**).

Activation of MeA Ucn3 neurons increases interest in novel conspecifics

To determine the behavioral effect of activation of Ucn3-expressing neurons during social interaction, we transduced MeA neurons of *Ucn3::Cre* mice with a vector carrying a double-*loxP*-flanked (floxed) inverted open reading frame encoding channelrhodopsin-2 (ChR2) fused to enhanced yellow fluorescent protein (DIO-ChR2-eYFP) using an adeno-associated-virus (AAV5). This resulted in ChR2-eYFP expression in MeA Ucn3$^+$ neurons (**Fig. 5a** and **Supplementary Fig. 8b**). To determine the efficiency and stability of optical stimulation of ChR2 Ucn3$^+$ neurons, we performed patch clamp recordings in acute brain slices from ChR2-expressing mice (**Fig. 5b–f**). We used current injection (2 ms, 700 pA) and optical stimulation (5 ms light pulses, 4 mW/mm^2) to examine the ability of Ucn3$^+$ neurons to sustain AP firing at stimulation frequencies ranging from 1 Hz to 100 Hz. All patched neurons fired an action potential in response to every stimulation at stimulation frequencies of up to 10 Hz for optical (475 nm, 5 ms, 4 mW mm^{-2}) as well as electrical stimulation (2 ms, 700 pA, $n = 6$ cells from 2 mice) (**Fig. 5d**). This demonstrated that optical excitation at stimulation frequencies of 10 Hz or lower can effectively drive neuronal firing in our system. Using cell-attached patch clamp recordings, we next verified that MeA Ucn3 neurons could continuously fire APs at 5 Hz for 20 min (**Fig. 5e,f**), as was necessary for the behavioral characterization. We found that the average number of APs fired by the MeA Ucn3 neurons in response to 20 ms illumination remained constant during the entire 20 min ($P = 0.99$; repeated measures ANOVA). While there was some variability in the number of APs per stimulation at the single-cell level, all MeA Ucn3 neurons fired at least one AP per stimulation during the entire 20-min period.

For *in vivo* experiments, MeA-cannulated mice (*Ucn3::Cre*$^+$, treatment; *Ucn3::Cre*$^-$, control) were bilaterally injected with AAV5-EF1α-DIO-ChR2-eYFP virus. Two weeks later, mice were tested in the social approach test for 20 min, while light pulses were delivered into the MeA (**Supplementary Movie 1** and **Supplementary Fig. 8a**). The light source was then turned off and behavior was recorded for an additional 20 min. During illumination, *Ucn3::Cre*$^+$ mice showed increased approach behavior toward novel mice compared to controls (**Fig. 5g**). Thus, the result of optogenetic activation of MeA Ucn3 cells resembles the results observed following pharmacological activation of MeA CRF-R2. This phenotype was abolished when treatment was preceded with MeA injection of Astressin 2B (**Fig. 5h**), indicating that the effects we observed were mediated by CRF-R2. Treated mice were similar to control mice in their nonsocial exploratory behavior (**Supplementary Fig. 8c,d**). Thus, the results of the dyadic social test suggest that activation of MeA CRF-R2 or Ucn3 neurons promotes social investigation of novel conspecifics while loss-of-function promotes social investigation of familiar conspecifics.

Altered CRF-R2 expression in mouse models of social avoidance

The results we presented strongly suggest that the MeA Ucn3–CRF-R2 circuit is important in socioemotional balance and may be dysregulated in mouse models of social avoidance. We therefore measured the *Ucn3* and *Crfr2* gene expression levels in the MeA

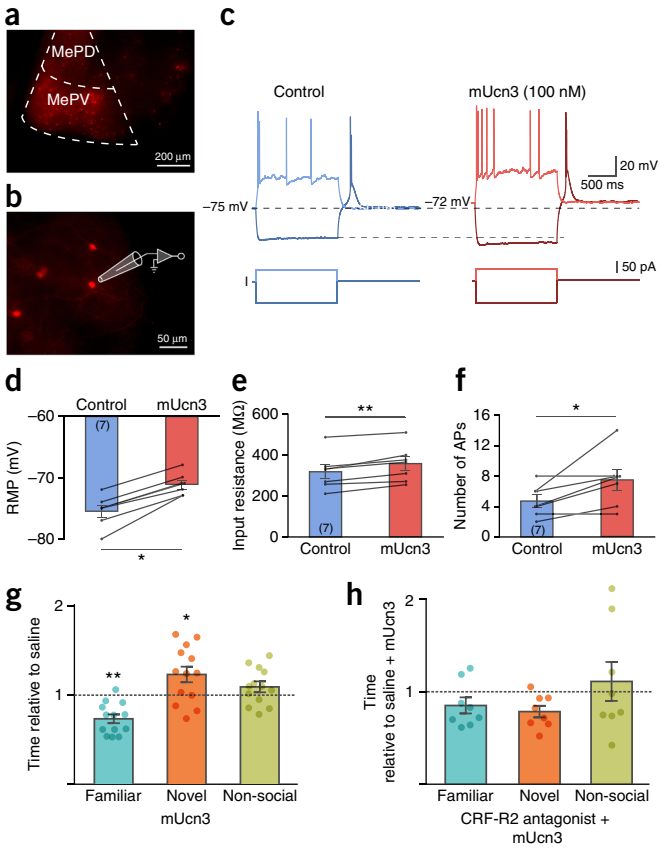

Figure 4 mUcn3 increases excitability of MeA CRF-R2 neurons, as well as preference for novel conspecifics. (**a**,**b**) Visualization of *Crfr2::Ai9* neurons in the medial amygdala (MeA). (**a**) Photomicrograph of an acute slice containing the MeA (postero-dorsal MeA (MePD) and postero-ventral MeA (MePV) portions) from a *Crfr2::Ai9* mouse ($n = 5$ mice). (**b**) Photomicrograph of the MePV portion of the slice showing a recorded cell ($n = 5$ mice). (**c**) Effects of a bath application of mUcn3 on CRF-R2 expressing neurons. Representative traces of the recorded neuron are shown under control conditions (blue traces) and 10 min after the bath application of mUcn3 (100 nM; red traces); mUcn3 caused a depolarization of the cell, increased the firing rate and increased the neuronal input resistance. The bottom traces represent the hyperpolarizing and depolarizing current injections ($n = 7$ cells from 5 mice). (**d**–**f**) Quantification of Ucn3 effects on CRF-R2 expressing neurons. mUcn3 induced a depolarization (**d**; resting membrane potential, –75.4 ± 0.9 mV under control conditions vs. –71.1 ± 0.6 mV in the presence of mUcn3, Wilcoxon two-tailed matched-pairs signed rank test, $P = 0.016$, $W = 28$, d.f. = 6), an increase in the input resistance (**e**; 319.0 ± 33.5 MΩ under control conditions vs. 355.7 ± 33.1 MΩ in the presence of mUcn3, paired two-tailed *t*-test, $P = 0.002$, $t = 5.45$, d.f. = 6), and an increase in AP firing (**f**; 4.7 ± 0.8 APs under control conditions vs. 7.4 ± 1.3 APs in the presence of Ucn3, paired two-tailed *t*-test, $P = 0.04$, $t = 5.454$, d.f. = 6) of CRF-R2 expressing neurons under control conditions (blue) and after bath application of mUcn3 (red) and the values for each individual recorded neuron ($n = 7$ cells from 5 mice). (**g**) The time spent by MeA mUcn3-administered mice ($n = 11$) in each chamber, presented relative to saline-injected control mice ($n = 13$). The MeA mUcn3 mice differed from controls in the amount of time spent in each chamber (RM one-way ANOVA, $P = 0.0009$, $F(2) = 9.759$). The MeA mUcn3 mice spent significantly less time investigating a familiar mouse (one-tailed *t*-test, $P = 0.0024$, $t = 3.42$, d.f. = 22) and more time investigating a novel mouse (one-tailed *t*-test, $P = 0.0258$, $t = 2.059$, d.f. = 22) compared to controls. (**h**) The time spent by CRF-R2 antagonist + mUcn3 mice ($n = 8$) in each chamber relative to control (saline + mUcn3) mice ($n = 12$). The CRF-R2 antagonist + mUcn3 mice did not differ from controls in the time they spent in each chamber (RM one-way ANOVA, $P = 0.2645$, $F(2) = 1.464$). Data are mean ± s.e.m. *n* is the number of animals, $^*P < 0.05$, $^{**}P < 0.01$.

in two common mouse models of social avoidance: chronic social defeat, an environmentally induced social avoidance model in which a test mouse is subjected to an aggressive bully mouse for 10 consecutive days (**Supplementary Fig. 9a**)[33], and the *Shank3* knockout mouse[34], a genetic model of social avoidance and autism-like behavior (**Supplementary Fig. 9b**). In both models, *Crfr2* mRNA levels were significantly downregulated in the MeA (**Fig. 6a**,**b**), while *Ucn3* levels remained unchanged (data not shown). These findings suggest the possible relevance of the MeA Ucn3–CRF-R2 circuit in both environmentally and genetically induced susceptibility to social avoidance in mice.

Inhibition of MeA Ucn3 neurons in a group elicits pro-social change

Mice, like humans, form groups with complex social dynamics[17]. Thus, strictly controlled tests, observing social interactions between pairs of mice[14], might be of limited ethological significance. To gain further insight into the role of the MeA Ucn3–CRF-R2 in regulation of relevant behaviors, we manipulated this circuit in an ethologically relevant environment. We used a behavioral system that allows tracking of multiple animals in an enriched environment under a 12-h light/12-h dark cycle over several days, with high temporal and spatial resolution[17] (**Supplementary Movies 2** and **3** and **Supplementary Fig. 10a**).

We hypothesized that in groups of littermates, where all members are familiar, inhibition of MeA Ucn3 cells would enhance social interaction, in agreement with the results from the dyadic experiments. To quantify interindividual and group interactions, we developed an image processing algorithm to automatically identify behaviors such as approaches and aggressive chases, which we used to infer the dominance hierarchy in the group.

To manipulate noninvasively the activity of MeA Ucn3$^+$ neurons within a group of mice, we used the DREADD system[35]. DREADDs are engineered G-protein-coupled receptors that can be selectively activated by the otherwise inert clozapine-*N*-oxide (CNO) administrated through the drinking water. To functionally validate the DREADD activity expressed in the MeA of *Ucn3::Cre*$^+$ mice, we measured cFos expression in the MeA following acute CNO administration. We found that cFos expression in the MeA of *Ucn3::Cre*$^+$ mice was significantly reduced (**Supplementary Fig. 10b**,**c**).

For the group behavior experiment, each group of four adult male mice (*Ucn3::Cre*$^+$, treatment mice; *Ucn3::Cre*$^-$, control mice) were injected bilaterally in the MeA with the conditional inhibitory DREADD virus (AAV8-hSyn-DIO-hM4D-mCherry; **Fig. 7a**) and, following 2 weeks of recovery, each group was introduced into the arena for a 7-d session. Following 1 d of habituation (day 0), behavior was recorded for 6 consecutive days during the dark phase. Starting from the fourth day, CNO was added to the drinking water until the sixth day (**Supplementary Fig. 10a**). This manipulation inhibited MeA Ucn3 neurons in treatment groups only (MeA *Ucn3::Cre*$^+$).

A fundamental property of many social groups is organization into hierarchical structures. In nature social dominance is frequently determined by fighting among members of the group, which in turn determines access to mating opportunities, food, and territory[36]. We therefore used the number of aggressive events between pairs of mice (which were automatically detected and classified by the

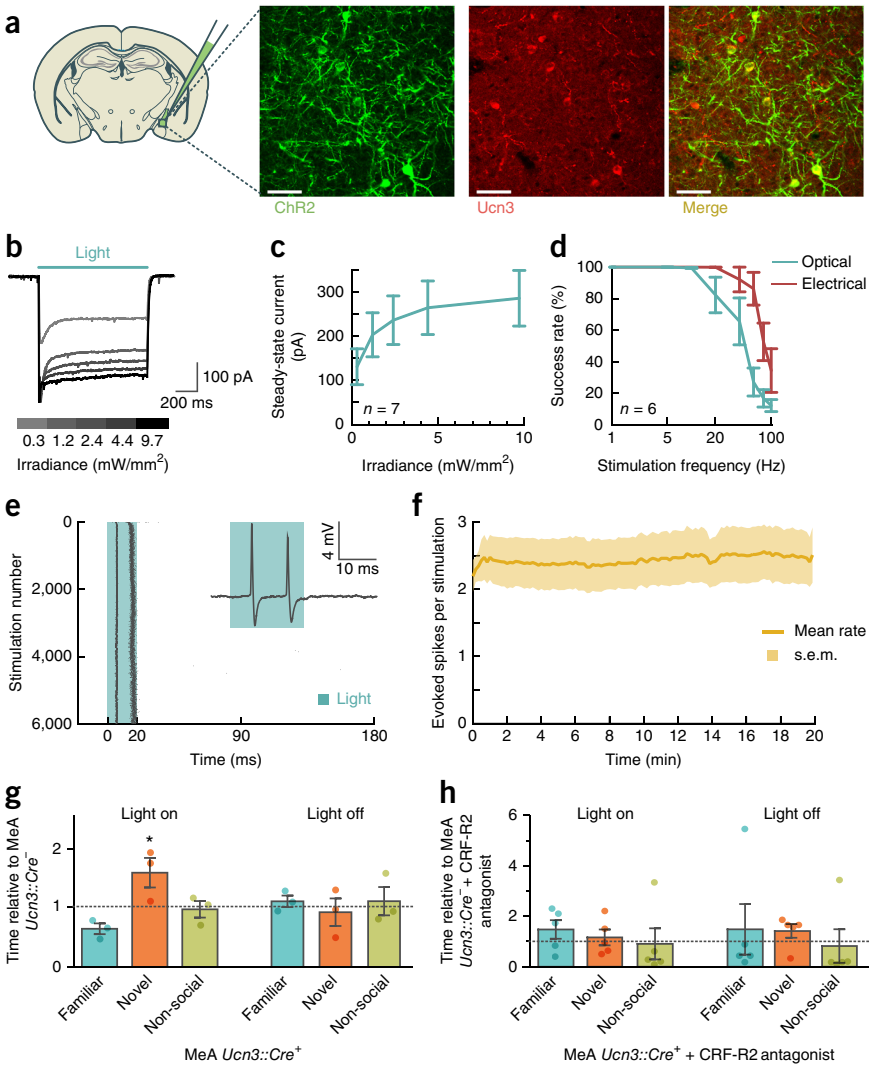

Figure 5 Optogenetic activation of MeA Ucn3 cells recapitulates the MeA CRF-R2 pharmacologic activation phenotype. (**a**) ChR2 is specifically expressed in MeA-Ucn3 neurons. Images depict the co-localization of ChR2-eYFP fluorescence (green) with anti-Ucn3 antibody (red) in the MeA. Scale bars represent 50 µm ($n = 3$ mice). (**b**–**f**), Electrophysiological confirmation of optogenetic activation of *Ucn3-ChR2*-expressing MeA neurons in acute brain slices. (**b**,**c**) Irradiance vs. steady state current during 1 s illumination. Photocurrents recorded in ChR2-expressing Ucn3 MeA cells were positively correlated with light power (RM ANOVA, $P = 5 \times 10^{-10}$, $F(4,24) = 37.74$, $n = 7$ cells from 2 mice). (**d**) Efficacy of spike triggering by optical and electrical stimulation with increasing stimulation frequency. All patched neurons reliably followed stimulation frequencies of up to 10 Hz for optical (475 nm, 5 ms, 4 mW mm^{-2}) as well as electrical stimulation (2 ms, 700 pA, $n = 6$ cells from 2 mice). (**e**) A raster plot of all APs fired during 20 min of optical stimulation at 5 Hz (470 nm, 20 ms, 5 mW mm^{-2}), measured by patch clamp recording in cell-attached configuration. Inset depicts a representative current clamp recording trace. (**f**) Quantification of **e** shows stability in evoked action potentials over 20 min of stimulation (repeated measures ANOVA, $F(119,714) = 0.7$, $P = 0.99$, $n = 7$). (**g**) The time spent by MeA *Ucn3::Cre*$^+$ mice ($n = 3$) in each chamber, presented relative to MeA *Ucn3::Cre*$^-$ control mice ($n = 4$). The MeA Ucn3$^+$ mice did not spend the same amount of time as controls in each chamber (RM two-way ANOVA, $P = 0.0197$, $F(2,4) = 12.25$). The MeA Ucn3$^+$ mice spent significantly more time investigating the novel mouse (one-tailed *t*-test, $P = 0.0435$, $t = 2.125$, d.f. = 5) compared to controls. Light on: 473 nm, 20 ms pulses, 5 Hz. (**h**) Delivery of CRF-R2 antagonist before optogenetic activation of MeA Ucn3 cells. The time spent by MeA *Ucn3::Cre*$^+$ mice ($n = 5$) in each chamber, presented relative to MeA *Ucn3::Cre*$^-$ control mice ($n = 5$). The MeA *Ucn3::Cre*$^+$ mice did not differ from MeA *Ucn3::Cre*$^-$ controls (RM two-way ANOVA, $P = 0.95$, $F(2, 8) = 0.05$). Data in **c**,**d**,**g**,**h** are mean ± s.e.m. *n* is the number of animals, $^*P < 0.05$, $^{**}P < 0.01$, $^{***}P < 0.001$.

system; see Online Methods) to infer the hierarchy. **Figure 7b** shows the group hierarchy as a graph with the minimum number of levels that preserves relative ranking between mice. Although the groups differed considerably in their hierarchical structure (**Fig. 7b**), the individual ranking of a mouse within its group was mostly stable following the inhibition of the Ucn3 neurons in the MeA(**Fig. 7c**).

Despite the stability of social organization, we found an enhancement in the pro-social behavior of the mice following hM4D-mediated silencing of MeA Ucn3 neurons. Compared with control mice, hM4D-expressing mice spent more time outside the nest, scouting the territory—a resource typically dominated by the alpha male[36] (**Fig. 7d**). In addition, we found a significant increase in the number of approaches (**Fig. 7e**). During the third day, in the hM4D-expressing mice, dominant mice approached subordinates more than vice versa, and group members of similar social rank approached each other the least (**Fig. 7f**). By contrast, in these groups, during the first day of CNO administration (the fourth day overall), approaches made toward individuals of similar social rank became most prominent, but there was no significant change in approaches toward subordinates or higher rank mice (**Fig. 7f**).

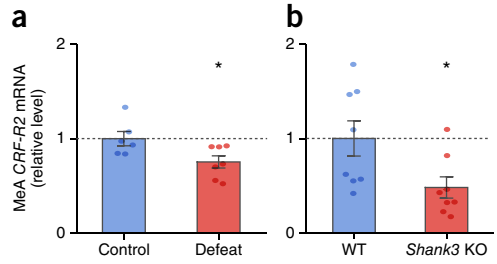

Figure 6 Reduced MeA *Crfr2* mRNA levels in mouse models of social avoidance. (**a**,**b**) In both models, *Crfr2* mRNA levels were significantly downregulated in the MeA. (**a**) Chronic social defeat (two-tailed Mann Whitney test, $P = 0.0221$ $U = 6$, d.f. = 12, treatment, $n = 6$ mice; control, $n = 7$ mice). (**b**) *Shank3* (two-tailed Mann Whitney test, $P = 0.028$, $U = 11$, d.f. = 15; WT, $n = 8$; KO, $n = 8$). Data are mean ± s.e.m. *n* is the number of animals.

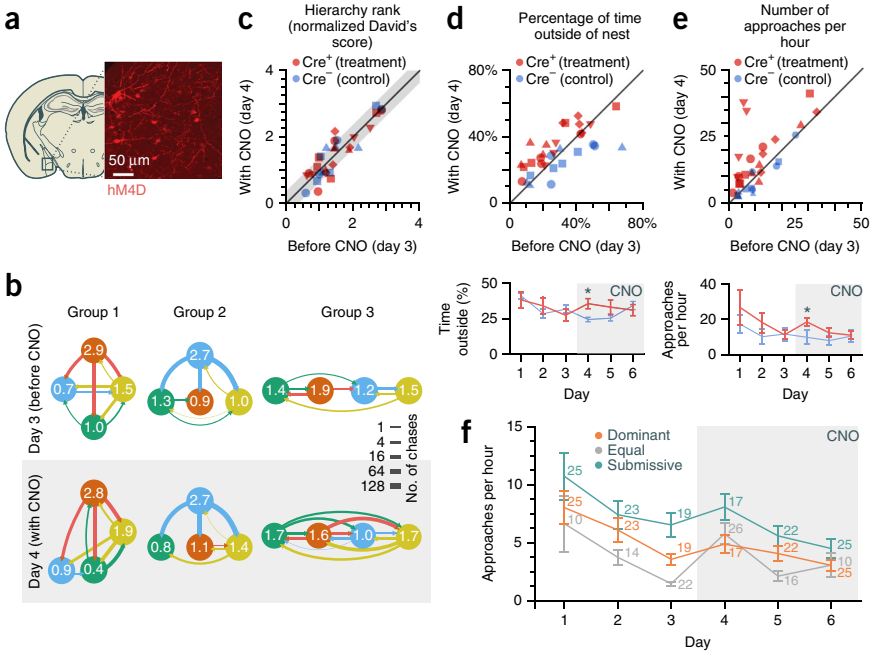

Figure 7 Inhibition of MeA Ucn3 neurons induces a pro-social change in individual preferences within a group of mice. (**a**) Within groups of 4 *Ucn3::Cre* 9-week-old male mice, each member was injected bilaterally in the MeA with conditional DREADD virus (hM4D). $n = 5$ mice. (**b**) Examples of group hierarchy maps (3 groups out of 5), based on aggressive contacts during day 3 (before CNO) and day 4 (during CNO) of the experiment (Online Methods). Graph nodes, mice; edges between nodes, number of chase-escape events between each pair. Edge width is proportional to the number, and color reflects the chaser. The number inside each node represents the dominance rank according to the normalized David's score (Online Methods). (**c**) Comparison of social rank, using the normalized David's score, before (*x*-axis, day 3) and during CNO administration (*y*-axis, day 4; Online Methods). Each colored dot represents one mouse, and shapes correspond to different groups (5 treatment Cre$^+$ groups totaling 20 mice, and 3 control Cre$^-$ groups totaling 12 mice). For validation, the interactions on the third day were randomly permuted into two sets several times, and a David's score was assigned to each individual independently for each set. Shaded area, s.d. of the differences in David's score between each pair of sets. The differences in normalized David's scores were not significant (two-tailed permutation test, treatment $P = 1.0$, control $P = 0.88$). (**d**) Change in the percentage of time the mice spent outside of the nest before and while CNO was added to the drinking water. The treatment groups showed a significant increase in the time outside (two-tailed permutation test, $P = 0.001$, $n = 20$), while the control groups spent more time inside the nest (two-tailed permutation test, $P = 0.015$, $n = 12$). Bottom panel: the amount of the time mice spent outside of their nests for each day of the experiment until CNO administration ceased (error bars indicate s.e.m.). Differences between the treatment and control groups following CNO administration were significant (two-tailed permutation test, $P = 0.049$, $n = 20$ and 12 respectively). (**e**) Comparison of the number of approaches each mouse performed toward another mouse that ended in a contact. Cre$^+$ mice made more approaches following CNO administration (two-tailed permutation test, $P = 0.001$, $n = 20$), whereas Cre$^-$ mice did not change their approach rate significantly (two-tailed permutation test, $P = 0.077$, $n = 20$ and 12 respectively). Bottom panel: daily approach rate (error bars show s.e.m.). Differences between treatment and control groups following CNO administration were significant (two-tailed permutation, test $P = 0.036$, $n = 20$ and 12 respectively). (**f**) Changes during CNO administration in the number of approaches made toward a superior, an inferior and an equal according to the dominance hierarchy (error bars show s.e.m.). The number of approaches toward equals increased significantly (two-tailed permutation test, $P = 0.0001$, $n = 22$ and 26), while approaches to mice of different rank remained similar (permutation test, $P = 0.072$ and $P = 0.53$ $n = 20$ and 12 for approaches toward dominant and subordinate accordingly, $n = 19$ and 17 respectively).

DISCUSSION

Animal and human studies have put forward the hypothesis that chronic psychosocial stress may act as a risk factor for psychiatric disorders. Individuals having poor social competence and high social anxiety are at greater risk of developing psychopathology than normally developing individuals, both in childhood and in adult life[37,38]. However, from an evolutionary point of view, moderate levels of social apprehension are essential for ensuring safe and successful social engagement. Thus, maintaining a proper balance between the processing of social signals and emotional responses to social challenges is essential for normal social performance.

This study provides comprehensive evidence that the Ucn3 component of the CRF stress system and its action through CRF-R2 in the MeA play a fundamental role in coping with social challenges in mice. We found that germline KOs of *Ucn3* and its receptor *Crfr2* resulted in reduced interest in novel conspecifics, with the latter also increasing interest in familiars. Knockdown of *Crfr2* specifically in the MeA was sufficient to recapitulate the *Crfr2* KO phenotype. Furthermore, pharmacological activation of MeA CRF-R2 and optogenetic activation of MeA *Ucn3* cells both induced the opposite phenotype.

What would be the benefit of a circuit that differentially regulates interactions with familiar conspecifics and novel ones? The mouse is an opportunistic species that occupies a variety of habitats and has a very flexible social structures. In rich and complex environments, mice usually live in groups consisting of a few subordinate males and breeding and nonbreeding females, all dominated by a single male[36]. The tolerance of the dominant male to intruders or to in-group subordinates varies widely and depends on the structure of the habitat[36]. Thus, the constant social challenge that is imposed by interactions between in-group members differs from challenges of acute interactions with invaders[15] and, accordingly, ways of coping with each challenge should be different.

Revealing the ethological significance of behavioral phenotypes observed in animal models is an important step toward translation of complex behavioral traits to endophenotypes that are relevant to humans. Using our dyadic social test, we found that inhibiting the MeA Ucn3–CRF-R2 circuit increased the mouse's interest in familiar conspecifics. Studying quantitatively the behavior of groups of mice in a semi-natural environment, we found that for a group of familiars, subchronic inhibition of MeA Ucn3 cells promoted tolerance and nonaggressive behaviors. Our combined approach of controlled short behavioral tests with ethologically relevant measurements of behavior has proven insightful in our quest to reveal mechanisms that underlie complex behaviors such as coping with social stress. Further refinement of this approach will advance the ability to assess the behavioral consequences of manipulating neural circuits[39].

Our findings also suggest how the MeA Ucn3–CRF-R2 circuit is embedded within a larger social brain network. We found that this circuit projects to and receives projections from brain areas that have been previously reported to be involved in regulation of social behavior,

including the BNST, LS, PVN, and PVT[10]. Such a network would probably be regulated by many neurotransmitters and neuromodulators. For example, the PVN, which we found received projections from both the MeA Ucn3 and CRF-R2 cells, is a region producing and secreting arginine vasopressin and oxytocin[26]. It has been reported that oxytocin not only motivates in-group favoritism, but also has a role in the emergence of intergroup conflict and violence[40]. Thus, the MeA Ucn3–CRF-R2 circuit is part of a complex network that regulates a range of complex social phenotypes.

Finally, the reduction in expression levels of MeA *Crfr2* mRNA in both an environmental model and a genetic model of social disorders in mice points to a possible involvement of stress system components in the amygdala in core symptoms of autism in humans, as well as in social deficits in other psychopathologies, such as social anxiety disorder[41] and schizophrenia.

METHODS

Methods, including statements of data availability and any associated accession codes and references, are available in the online version of the paper.

Note: Any Supplementary Information and Source Data files are available in the online version of the paper.

ACKNOWLEDGMENTS

We thank S. Ovadia for his devoted assistance with animal care. We thank J. Keverne for professional English editing, formatting and scientific input. This work is supported by an FP7 grant from the European Research Council (260463; A.C.); research grants from the Israel Science Foundation (1565/15) (A.C.); research support from Roberto and Renata Ruhman (A.C.); research support from Bruno and Simone Licht; I-CORE Program of the Planning and Budgeting Committee and The Israel Science Foundation (grant no. 1916/12 to A.C.); the Nella and Leon Benoziyo Center for Neurological Diseases (A.C.); the Henry Chanoch Krenter Institute for Biomedical Imaging and Genomics (A.C.); the Perlman Family Foundation, founded by Louis L. and Anita M. Perlman (A.C.); the Adelis Foundation (A.C.); the Irving I. Moskowitz Foundation (A.C.); grants from the Israel Science Foundation (1351/12) and the European Commission (ERC StG #337637 and Marie Curie CIG #321919) (O.Y.) and a Human Frontier Program career development award (O.Y.); a Human Frontier Science Program grant (E.S.); European Research Council grant # 311238 (E.S.); an Israel Science Foundation grant #1629/12 (E.S.); research support from Martin Kushner Schnur (E.S.); and Mr. and Mrs. Lawrence Feis (E.S.).

AUTHOR CONTRIBUTIONS

Y. Shemesh and O.F. designed and performed most of the experiments. M.M., M.E., J.D., and J.M.D. designed and performed electrophysiological studies. S.A., S.M., T.S., E.E., L.T., G.E., E.S.A., Y.J.B.-E., S.G., Y.K., and S.H. assisted in experiments. Y. Shemesh, Y. Sztainberg, and O.F. wrote the code for analyzing behavior and validated it. E.S., O.Y., and A.C. conceived, designed, and supervised the project. Y. Shemesh, O.F., and A.C. wrote the manuscript.

COMPETING FINANCIAL INTERESTS

The authors declare no competing financial interests.

1. Tost, H., Champagne, F.A. & Meyer-Lindenberg, A. Environmental influence in the brain, human welfare and mental health. *Nat. Neurosci.* **18**, 1421–1431 (2015).
2. Iarocci, G., Yager, J. & Elfers, T. What gene-environment interactions can tell us about social competence in typical and atypical populations. *Brain Cogn.* **65**, 112–127 (2007).
3. Heimberg, R.G. *et al.* Social anxiety disorder in DSM-5. *Depress. Anxiety* **31**, 472–479 (2014).
4. Mehling, M.H. & Tassé, M.J. Severity of autism spectrum disorders: current conceptualization, and transition to DSM-5. *J. Autism Dev. Disord.* **46**, 2000–2016 (2016).
5. Eisenberger, N.I. & Cole, S.W. Social neuroscience and health: neurophysiological mechanisms linking social ties with physical health. *Nat. Neurosci.* **15**, 669–674 (2012).
6. Sztainberg, Y. & Chen, A. Neuropeptide regulation of stress-induced behavior: insights from the crf/urocortin family. in *Handbook of Neuroendocrinology* (eds Fink, G., Pfaff, D.W. & Levine, J.) Ch. 15 (Academic Press, 2011).
7. Lewis, K. *et al.* Identification of urocortin III, an additional member of the corticotropin-releasing factor (CRF) family with high affinity for the CRF2 receptor. *Proc. Natl. Acad. Sci. USA* **98**, 7570–7575 (2001).
8. Deussing, J.M. *et al.* Urocortin 3 modulates social discrimination abilities via corticotropin-releasing hormone receptor type 2. *J. Neurosci.* **30**, 9103–9116 (2010).
9. Van Pett, K. *et al.* Distribution of mRNAs encoding CRF receptors in brain and pituitary of rat and mouse. *J. Comp. Neurol.* **428**, 191–212 (2000).
10. Goodson, J.L. The vertebrate social behavior network: evolutionary themes and variations. *Horm. Behav.* **48**, 11–22 (2005).
11. Brennan, P.A. & Keverne, E.B. Something in the air? New insights into mammalian pheromones. *Curr. Biol.* **14**, R81–R89 (2004).
12. Samuelsen, C.L. & Meredith, M. Categorization of biologically relevant chemical signals in the medial amygdala. *Brain Res.* **1263**, 33–42 (2009).
13. Toth, I. & Neumann, I.D. Animal models of social avoidance and social fear. *Cell Tissue Res.* **354**, 107–118 (2013).
14. Silverman, J.L., Yang, M., Lord, C. & Crawley, J.N. Behavioural phenotyping assays for mouse models of autism. *Nat. Rev. Neurosci.* **11**, 490–502 (2010).
15. Gray, S.J., Jensen, S.P. & Hurst, J.L. Structural complexity of territories: preference, use of space and defence in commensal house mice, *Mus domesticus*. *Anim. Behav.* **60**, 765–772 (2000).
16. Kalueff, A.V., Wheaton, M. & Murphy, D.L. What's wrong with my mouse model? Advances and strategies in animal modeling of anxiety and depression. *Behav. Brain Res.* **179**, 1–18 (2007).
17. Shemesh, Y. *et al.* High-order social interactions in groups of mice. *Elife* **2**, e00759 (2013).
18. de Chaumont, F. *et al.* Computerized video analysis of social interactions in mice. *Nat. Methods* **9**, 410–417 (2012).
19. Hong, W. *et al.* Automated measurement of mouse social behaviors using depth sensing, video tracking, and machine learning. *Proc. Natl. Acad. Sci. USA* **112**, E5351–E5360 (2015).
20. Moy, S.S. *et al.* Social approach in genetically engineered mouse lines relevant to autism. *Genes Brain Behav.* **8**, 129–142 (2009).
21. Watabe-Uchida, M., Zhu, L., Ogawa, S.K., Vamanrao, A. & Uchida, N. Whole-brain mapping of direct inputs to midbrain dopamine neurons. *Neuron* **74**, 858–873 (2012).
22. Allen Institute for Brain Science. *Allen Mouse Brain Atlas.* http://mouse.brain-map.org (2015).
23. Lein, E.S. *et al.* Genome-wide atlas of gene expression in the adult mouse brain. *Nature* **445**, 168–176 (2007).
24. Wesson, D.W. & Wilson, D.A. Sniffing out the contributions of the olfactory tubercle to the sense of smell: hedonics, sensory integration, and more? *Neurosci. Biobehav. Rev.* **35**, 655–668 (2011).
25. Lebow, M.A. & Chen, A. Overshadowed by the amygdala: the bed nucleus of the stria terminalis emerges as key to psychiatric disorders. *Mol. Psychiatry* **21**, 450–463 (2016).
26. Stoop, R. Neuromodulation by oxytocin and vasopressin. *Neuron* **76**, 142–159 (2012).
27. Lo, L. & Anderson, D.J.A. A Cre-dependent, anterograde transsynaptic viral tracer for mapping output pathways of genetically marked neurons. *Neuron* **72**, 938–950 (2011).
28. Pardo-Bellver, C., Cádiz-Moretti, B., Novejarque, A., Martínez-García, F. & Lanuza, E. Differential efferent projections of the anterior, posteroventral, and posterodorsal subdivisions of the medial amygdala in mice. *Front. Neuroanat.* **6**, 33 (2012).
29. Taniguchi, H. *et al.* A resource of Cre driver lines for genetic targeting of GABAergic neurons in cerebral cortex. *Neuron* **71**, 995–1013 (2011).
30. Kirouac, G.J. Placing the paraventricular nucleus of the thalamus within the brain circuits that control behavior. *Neurosci. Biobehav. Rev.* **56**, 315–329 (2015).
31. Lebow, M. *et al.* Susceptibility to PTSD-like behavior is mediated by corticotropin-releasing factor receptor type 2 levels in the bed nucleus of the stria terminalis. *J. Neurosci.* **32**, 6906–6916 (2012).
32. Keshavarzi, S., Sullivan, R.K., Ianno, D.J. & Sah, P. Functional properties and projections of neurons in the medial amygdala. *J. Neurosci.* **34**, 8699–8715 (2014).
33. Elliott, E., Ezra-Nevo, G., Regev, L., Neufeld-Cohen, A. & Chen, A. Resilience to social stress coincides with functional DNA methylation of the Crf gene in adult mice. *Nat. Neurosci.* **13**, 1351–1353 (2010).
34. Peça, J. *et al.* Shank3 mutant mice display autistic-like behaviours and striatal dysfunction. *Nature* **472**, 437–442 (2011).
35. Urban, D.J. & Roth, B.L. DREADDs (designer receptors exclusively activated by designer drugs): chemogenetic tools with therapeutic utility. *Annu. Rev. Pharmacol. Toxicol.* **55**, 399–417 (2015).
36. Bronson, F.H. The reproductive ecology of the house mouse. *Q. Rev. Biol.* **54**, 265–299 (1979).
37. Selten, J.-P., van der Ven, E., Rutten, B.P. & Cantor-Graae, E. The social defeat hypothesis of schizophrenia: an update. *Schizophr. Bull.* **39**, 1180–1186 (2013).
38. van Os, J., Kenis, G. & Rutten, B.P. The environment and schizophrenia. *Nature* **468**, 203–212 (2010).
39. Anderson, D.J. & Perona, P. Toward a science of computational ethology. *Neuron* **84**, 18–31 (2014).
40. De Dreu, C.K., Greer, L.L., Van Kleef, G.A., Shalvi, S. & Handgraaf, M.J. Oxytocin promotes human ethnocentrism. *Proc. Natl. Acad. Sci. USA* **108**, 1262–1266 (2011).
41. Miskovic, V. & Schmidt, L.A. Social fearfulness in the human brain. *Neurosci. Biobehav. Rev.* **36**, 459–478 (2012).

ONLINE METHODS

Animals. In all experiments we used male mice. *Crfr2* KO mice and *Ucn3* KO mice were generated on a mixed C57BL/6X129 background. For both the *Crfr2* KD experiments and the pharmacology experiments, we used C57BL/6J male mice (Harlan Laboratories, Jerusalem, Israel). *Ucn3*::*Cre* mice were obtained from GENSAT (congenic on C57BL/6 background; involves C57BL/6, FVB/N, ICR and unspecified strains). Mice were kept in groups of 4 or 5 animals per cage and were 9–11 weeks old during the experiments. Throughout the experiments, the animals were maintained in a temperature-controlled room (22 ± 1 °C) on a reverse 12 h light–dark cycle. Food and water were given *ad libitum*. All experimental protocols were approved by the Institutional Animal Care and Use Committee of the Weizmann Institute of Science.

Behavioral assessments. *Social approach test.* The maze is made of gray PVC (see **Fig. 1a** and **Supplementary Movie 1**). Its walls (25 cm high) are inclined outwards by 10° and its center is a 15 × 15 cm chamber. Each of its three arms is divided in the middle into two more chambers (15 × 30 cm each). The chambers that are close to the center are connected to it by a small 2.5 × 2.5 cm hole (passage is open for the optogenetics experiments). The lower 5-cm part of each middle-arm-divider is a mesh, made of four gaps, each a 1-cm-wide strip, through which the conspecific mice can communicate through tactile and odor cues. Illumination at the bottom of the arena is 1 lx and the test lasts 30 min. For videotaping and analysis, we used the automated video tracking system Ethovision 7.0 (Noldus, Wageningen, the Netherlands).

Habituation: On 2 consecutive days before the test, the actor was placed alone in the center chamber and was allowed to explore the center and the first chamber of each arm for 30 min. Subsequently, each conspecific (familiar and novel) was placed in one of the chambers at the far end of the maze arms for 30 min.

Test: The actor was placed in the center of the arena and allowed to explore it and the adjacent chambers for 20 min. It was then confined to the center chamber while the novel and familiar mice were placed in their chambers; subsequently the actor was released to move freely in the maze. In each trial different conspecifics were used. **Supplementary Figure 11** depicts the baseline behavior of the control groups in the various experiments.

Anxiety-like behaviors. All behavioral assessments were performed during the dark phase following habituation to the test room for 2 h before any test. For the assessment of anxiety-like behaviors, we used the open field (OF) and the dark–light transfer (DLT) tests. The OF consisted of an acrylic glass box (50 × 50 × 22 cm). The arena was illuminated with 120 lx. Each mouse was placed in the corner of the apparatus to initiate a 10-min test session. The time spent in the center of the arena, the latency to cross the center, and the number of entries into the center of the arena were measured. The DLT test consisted of two compartments, a dark one (14 × 27 × 26 cm) and a 1,050-lx illuminated light compartment (30 × 27 × 26 cm), connected by a small passage. The mice were placed in the dark compartment to initiate a 5-min test session. The time spent in the light compartment, the number of entries into the light compartment and the latency of entering the light zone were measured. The indices collected in these tests were quantified using an automated video tracking system (VideoMot2; TSE Systems, GmbH, Bad Homburg, Germany).

*Locomotor activity***.** Locomotor activity was examined over a 3-d period. Mice were singly housed in specialized home cages, and locomotion was measured using an infrared-based automatic system (InfraMot; TSE Systems GmbH, Bad Hamburg, Germany).

Novel object preference. The novel object preference test was performed in a gray PVC arena, divided into three chambers and connected by small portholes through which the mice could pass. Illumination at the bottom of the arena was 2 lx. The Observer XT (Noldus, Wageningen, the Netherlands) was used for videotaping and analysis. Objects were pencil sharpeners, approximately 6 cm high. There were 2 d of a 1-min handling session before habituation days. Prior to test day, there were 3 habituation days. In the first habituation day, the mice explored the empty chambers for 10 min, and then they were returned to their cage for a 10 min intertrial interval (ITI) followed by 10 min of familiarizing themselves with two identical objects, one object placed in one of the each of the outer chambers. The next two habituation days were the same, except that the two identical objects were present at both trials. On test day, the second trial lasted only 5 min and the mouse was placed in the center chamber with the familiar object in one outer chamber and a new object in the other outer chamber. The time the mouse's nose was within 2 cm of each object and also directed toward it was calculated.

Chronic social defeat. The social defeat protocol was carried out as previously described[33]. An 8-week-old C57/Bl test mouse was placed in the home cage of an aggressive ICR retired breeder mouse, and they interacted physically for 5 min. During this time, the ICR mouse attacked the intruder mouse. After the 5-min attack period, a perforated clear acrylic glass divider was placed between the animals and they remained in the same cage for 24 h to allow sensory contact. The procedure was then repeated by placing the test mouse with an unfamiliar ICR mouse for each of the next 10 d, allowing a 5-min attack period and 24-h sensory contact period. Unstressed mice were housed two mice per cage, with a divider between them. After the 10-d protocol, stressed mice were housed for an additional 2 weeks, at two stressed mice per cage, to test for long-term effects of chronic social defeat, and then mice were killed for analysis.

Acute social defeat for DREADD validation. All animals underwent social defeat during a 5-min encounter with an aggressive ICR mouse. After the 5-min attack period, a perforated clear acrylic glass divider was placed between the animals for 90 min. Subsequently animals were perfused and brain sections were stained for cFos (the product of the early immediate gene *Fos*). Five animals received IP injection of CNO before the social defeat, while four animals received a saline injection (control).

Real-time PCR. Mice were killed by rapid decapitation and brains were quickly removed. The medial amygdala was isolated on dry ice and then stored at −80 °C until mRNA extraction. Total mRNA was purified using PerfectPure tissue RNA kit (5 Prime GmbH, Hilden, Germany). cDNA was synthesized from RNA samples using the High Capacity cDNA Reverse Transcriptase kit (Applied Biosystems, Waltham, MA, USA). Real-time PCR was performed using FastStart Universal SYBR Green Master (Rox) (Roche Diagnostics, Indianapolis, IN, USA) and analyzed with a ViiA7 Real-Time PCR System (Applied Biosystems, Waltham, MA, USA). Technical triplicates were performed on each biological sample. The primers used were as follows: HPRT forward, GCAGTACAGCCCCAAAATGG; reverse, GGTCCTTTTCACCAGCAAGCT; CRF-R2 forward, TACCGAATCGCCCTCATTGT; reverse, CCACGCGAT GTTTCTCAGAAT. UCN3 forward, CTCCTGGCCCGGAAGC; reverse, CATCAGCATCGCTCCCTGT.

Lentiviral vector design, production and validation. The lenti-sh*Crfr2* vectors were designed as described previously[31]. In brief, four different short hairpin RNA (shRNA) target sequences from the open reading frame of the mouse *Crfr2* gene were cloned into shRNA expression cassettes driven by the H1 promoter in the p156RRLsinPPTCMV-GFP-PREU3Nhe lentiviral construct (kindly provided by Inder Verma, the Salk Institute for Biological Studies). The recombinant pseudotyped lentiviral vectors were generated by cotransfection of four plasmids into HEK293T cells, as described earlier[15]. The ability of lenti-sh*Crfr2* vectors to knock down *Crfr2* expression was assessed by western blot analysis as described previously[15].

Intracerebral injections of lentiviral vectors and AAVs. Twenty-four adult (9 weeks old) C57BL/6J male mice (Jackson Laboratory) received bilateral stereotaxic injections of lentivirus into the MeA (1 µl lentivirus per side, 0.3 ml min^{-1}). Twelve mice received the lenti-sh*Crfr2* and 12 mice received the control, irrelevant virus (*shUcn2*). Seventeen adult (9 weeks old) C57BL/6J male mice (3 *Ucn3*::*Cre*$^{+}$ and 4 *Ucn3*::*Cre*$^{-}$, Jackson Laboratory) received bilateral stereotaxic injections of AAV5-EF1α-DIO-ChR2-EYFP into the MeA (0.35 ml per side, 0.1 ml min^{-1}). Nine groups of C57BL/6J/ICR male mice (9 weeks old, 4 individuals per group: 6 *Ucn3*::*Cre*$^{+}$ groups and 3 *Ucn3*::*Cre*$^{-}$ groups) received bilateral stereotaxic injections of AAV8-hSyn-DIO-hM_4D-mCherry into the MeA (0.35 µl per side, 0.05 ml min^{-1}).

Mice were anesthetized with isoflurane and placed on a computer-guided stereotaxic instrument (Angle Two Stereotaxic Instrument, myNeurolab, Leica Microsystems Inc., Bannockburn, IL, USA), which is fully integrated with the Franklin and Paxinos mouse brain atlas through a control panel. The viral vectors were delivered using a Hamilton syringe connected to a motorized nanoinjector. To allow diffusion of the solution into the brain tissue, the needle was left in place for an additional 2 min after the injection (coordinates, relative to bregma: AP = −1.7 mm, L = ±2.25 mm, H = −5.3 mm, based on a calibration study indicating these coordinates as leading to the MeA in C57BL/6 strain). The mice were allowed to recover from the surgery for a period of 2 weeks before

behavioral testing. Following behavioral tests, confirmation of the accuracy of the injection site for the lenti-sh*Crfr2* was done by immunostaining using biotinylated anti-GFP antibody and for the AAV5-EF1α-DIO-ChR2-EYFP by EYFP expression.

For cell-type-specific retrograde tracing, AAV5-EF1a-FLEX-TVA-mCherry and AAV8-CAG-FLEX-RG were stereotaxically injected into the MeA. Two weeks later, 2 µl of pseudotyped rabies virus, SADΔG-GFP(EnvA), was injected into the same area. One week after injection of rabies virus, mice were perfused. We injected 6 *Ucn3::Cre*$^{+}$ mice with both the helpers and rabies viruses; 2 of the 6 showed clear EYFP expression in the injection site, and their brains were further analyzed for sites that project to the MeA. For cell-type-specific anterograde tracing, we used stereotaxic injection into the MeA of H129DTK-TT recombinant virus into the MeA. Mice were monitored daily for the development of symptoms: a slightly hunched back and increased anxiety. Mice showed such symptoms after 2 d and were immediately perfused. For observation of synapses originated from MeA Ucn3 neurons, 300 nl AAV9-CMV-Flex-synaptophysin-mCherry viral vector (McGovern Institute for Brain Research at MIT) was injected bilaterally into the MeA of *Ucn3::Cre*$^{+}$ mice. Mice were perfused 1 month after the injection.

Immunohistochemistry. Animals were anesthetized with chloral hydrate (1.4 g per kg body weight, intraperitoneally) and perfused transcardially with 100 ml of PBS followed by 100 ml of 4% paraformaldehyde in a borate buffer, pH 9.5. The brains were removed and post-fixed in 30% sucrose using the same fixative at 4 °C, frozen and sectioned coronally at 30 µm using a sliding microtome (Leica Microsystems GmbH, Wetzlar, Germany) and stored in PBS at 4 °C until used. Brain slices were blocked for 1 h with PBS containing 0.3% Triton and 20% normal horse serum to prevent nonspecific binding.

Verification of injection sites. Brain slices were incubated overnight at room temperature (RT) with rabbit anti-GFP antibody (1:100) as the primary antibody (MBL, Naka-ku, Japan, cat no. 598), followed by Cy2-conjugated secondary antibody (Chemicon-Millipore, Schwalbach, Germany, cat no. 16220084). The slices were then washed and mounted on gelatin-coated slides and screened using a fluorescent microscope for GFP expression at the injection sites. Representative images were captured. Mice that did not show GFP at the aimed injection location were excluded from the data.

Co-staining for Ucn3 and ChR2. Brain slices were incubated overnight at RT with goat anti-GFP biotin antibody (1:200, Abcam, cat no. ab6658) and rabbit anti-Ucn3 (1:500, kindly provided by the Vale laboratory, The Salk Institute for Biological Studies, La Jolla, CA)[8] as primary antibodies, followed by Cy2 streptavidin (1:200, Jackson ImmunoResearch, USA, cat no. 16220084) and Cy3 anti-rabbit (1:200 Jackson ImmunoResearch, USA, cat. no. 711165152).

Quantification of cFos expression. Brain slices were incubated overnight at RT with rabbit anti-cFos (1:1,000 Santa Cruz Biotechnology cat no. sc-52) followed by Alexa 594 anti-rabbit (1:200, Life Technologies, cat. no. A31632).

Images were captured using a confocal microscope (Zeiss LSM510 and LSM700) at 10× and 20× magnifications. Quantification of cFos-positive neurons was done using IMARIS software.

Double *in situ* hybridization. Double ISH procedures were performed as previously described[8]. *Crfr2::tdTomato*$^{+}$ male mice (10 weeks old) were killed in the early afternoon (14:00 h) by decapitation. Brains were carefully removed and immediately snap-frozen on dry ice. Frozen brains were cut on a cryostat into 20-µm-thick sections and mounted on SuperFrost Plus slides (Thermo Scientific Shandon, Fisher Scientific UK Ltd, Loughborough, UK). All sections were processed for ISH as described before[8]. The following riboprobes were used: *GAD65*: nucleotides 753–1600 of GenBank accession code NM_008078; *GAD67*: nucleotides 984–1940 of GenBank accession code NM_008077; *tdTomato*: nucleotides 337–1026 of GenBank accession code NM_205769. Specific DNA fragments encoding the riboprobes were generated by PCR applying T7 and T3 or SP6 primers using plasmids containing the above-mentioned cDNAs as templates. Antisense and sense cRNA probes were synthesized and labeled with [^{35}S]UTP or digoxigenin (DIG) by *in vitro* transcription with 200 ng of respective PCR product used as templates. For DIG detection, anti-DIG-POD (Fab) antibody (Roche, cat no. 11207733910) was used at 1:400. Tyramide-biotin signal amplification (TSA) was performed using the NEL700A Kit (PerkinElmer, Waltham, MA, USA) following the manufacturer's instructions. Dipping, development, and acquisition of the autoradiograms were performed as described before[8].

Bright-field photomicrographs were captured with a Zeiss Axioplan2 microscope (Göttingen, Germany). Images were digitalized using Axio Vision 4.9 (Zeiss, Göttingen, Germany), and photomicrographs were integrated into plates using image-editing software. Only sharpness, brightness and contrast were adjusted. Brain slices were digitally cut out and set onto an artificial white background.

Cannulation of animals. Mice were anesthetized with isoflurane and placed in a stereotaxic apparatus (Angle Two Stereotaxic Instrument with Mouse Atlas, MyNeurolab, Richmond, Illinois, USA). A midline incision was made across the top of the skull. After cleaning the periosteum, the vertical coordinates of bregma and lambda were measured to align in the same plane (level head). For MeA cannulation, a guide cannula (28 gauge; 5.5 tubing length below pedestal; Plastics One, Roanoke, VA, USA) was inserted bilaterally into the MeA (AP = −1.7 mm, L = ±2.6 mm, H = −5.1 mm ventral angle = 10°, relative to bregma). Cannulae were secured with C&B-Metabond kit (Parkell Inc., Edgewood, NY, USA) and Jet acrylic dental cement (Lang Dental Manufacturing Co., Wheeling, IL, USA). Removable dummy cannulae with tip extending 0.5 mm below the guide cannulae were placed in the guide cannulae to maintain patency until the time of injections. Animals received 30 µl durabiotics s.c. after surgery. Mice were allowed a minimum of 10 d to recover from surgery before any intracerebral microinjection. At the end of experiments, brains were sectioned to determine the placement of cannulae. Only animals with the tip of the cannula located at the MeA were included in the analysis. After the completion of behavioral testing, mice were overdosed with chloral hydrate 35% and perfused intracardially. The brains were removed, sectioned in the coronal plane at 30 µm thickness and Nissl stained.

Peptide preparation. The mUcn3 and Astressin-2B peptides were dissolved separately in BSA at 1 mg/ml (mUcn3: 187 µM; Astressin-2B: 241 µM) and stored at −20 °C. Immediately before each day of microinjection experiments, mUcn3 and Astressin-2B were dissolved separately in sterile aCSF to reach a concentration of 187 nM and 1.6 µM, respectively.

Drug administration. Mice were anesthetized with isoflurane, dummy cannulae were removed and an injection needle (33g) was inserted into the guide cannula. The injection needle was attached by a polyethylene tube to a 2-µl Hamilton syringe. The solution was injected with a volume of 0.5 µl, at a rate of 0.12 µl min^{-1}, to each side using a microinjection pump. Injections were followed by a waiting period of 3 min to ensure the full dose was delivered; control mice received 0.5 µl vehicle (artificial CSF). Immediately after the injections, mice were taken to the social maze for 20 min habituation followed by 30 min of social interaction test.

Optical stimulation. Two 1.65-m optical fibers (BFL37-200, Thorlabs, Newton, NJ, USA) were connected with FC connectors at one end and cleaved flat at the other end. The cleaved ends were epoxy-glued to the injector guide (Plastics One Inc., Roanoke, VA, USA) such that when both fibers were inserted fully into the bilateral guide cannulae, the cleaved ends of the fibers emerged ~0.5 mm past the end of the guide cannulae. The FC connectorized ends were attached to a 1x2i FC/PC Fiberoptic Rotary Joint (Doric Lenses, Québec, Canada), which was further FC-coupled to the light source (CrystaLaser, Reno, NV, USA).

The cleaved ends of the optical fibers were inserted through the guide cannulae into the MeA of the mouse immediately before, and removed immediately after, behavior testing. Light pulse trains (20Hz, 20ms) were programmed using a function generator (33220A, Agilent, Santa Clara, CA, USA) which was connected via cable to a 473 nm solid state laser diode source (CrystaLaser, Reno, NV, USA), as well as the optical fiber via a fiber coupler. The laser output at the end of the fiber was calibrated to 8 mW using a light power meter (Thorlabs, Newton, NJ, USA). Before fiber insertion, mice were briefly anaesthetized with isoflurane. Following anesthesia, mice were allowed to habituate to the behavioral apparatus for 20 min before behavioral testing.

Slice preparation. Mice were injected intraperitoneally with pentobarbital (130 mg/kg, i.p.) and perfused with carbogenated (95% O_2, 5% CO_2) ice-cold slicing solution (in mM: 2.5 KCl, 11 glucose, 234 sucrose, 26 $NaHCO_3$, 1.25 NaH_2PO_4, 10 $MgSO_4$, 2 $CaCl_2$; 340 mOsm). After decapitation, 300-µm coronal MeA slices were prepared in carbogenated ice-cold slicing solution using a

doi:10.1038/nn.4346

vibratome (Leica VT 1200S) and allowed equilibrate for 20 min at 33 °C in carbogenated high-osmolarity artificial cerebrospinal fluid (high-Osm ACSF; [mM] 3.2 KCl, 11.8 glucose, 132 NaCl, 27.9 $NaHCO_3$, 1.34 NaH_2PO_4, 1.07 $MgCl_2$, 2.14 $CaCl_2$; 320 mOsm) followed by 40 min incubation at 33 °C in carbogenated ACSF (in mM: 3 KCl, 11 glucose, 123 NaCl, 26 $NaHCO_3$, 1.25 NaH_2PO_4, 1 $MgCl_2$, 2 $CaCl_2$; 300 mOsm). Subsequently, slices were kept at RT in carbogenated ACSF until use. The recording chamber was perfused with carbogenated ACSF at a rate of 2 ml min^{-1} and maintained at 32 °C.

***In vitro* characterization of Ucn3 effect on CRF-R2-expressing neurons.** Acute brain slices from adult (8–10 weeks old) *Crfr2-tdTomato* mice were prepared as described above. All experiments were carried out at room temperature and slices were continuously superfused (4–5 ml/min) with ACSF containing 50 µM APV, 5 µM NBQX, 10 µM bicuculline methiodide, and 5 µM CGP 55845. Neurons of the postero-ventral subdivision of the MeA (MePV) expressing *Crfr2 tdTomato* were identified by epifluorescence microscopy. Afterwards, the cell bodies of these neurons were visualized by infrared videomicroscopy and the gradient contrast system. Somatic whole-cell patch-clamp recordings (seal resistance >1 GΩ) were performed in bridge mode using a discontinuous single-electrode voltage-clamp amplifier (SEC-10L, npi electronics, Tamm, Germany). Only measurements of the access resistance were done in voltage-clamp mode (holding potential −70 mV). The current/potential was low-pass filtered at 3 kHz, digitized at 9 kHz via an ITC-16 interface board, and stored with the standard software Pulse 8.31 (HEKA Elektronik, Lambrecht/Pfalz, Germany). The patch-clamp electrodes (open-tip resistance 4–5 MΩ) were pulled from borosilicate glass capillaries (Harvard Apparatus, Kent, UK) on a DMZ-Universal puller (Zeitz Instruments, Munich, Germany) and filled with a solution consisting of (in mM): 130 potassium gluconate, 5 NaCl, 2 $MgCl_2$, 5 D-glucose, 10 HEPES, 0.5 EGTA, 2 Mg-ATP, 0.3 Na-GTP, 20 phosphocreatine, pH 7.3 with KOH, osmolarity 305 mOsm. Electrophysiological measurements under control conditions were carried out 5 min after reaching the whole-cell configuration. The input resistance was calculated from steady-state voltage responses upon negative current injections (1,500 ms) where no 'sag' could be detected. Firing frequency was evaluated by positive current injections (400 ms) that induced mild firing (2–8 action potentials) of the neurons under control conditions. Ucn3 (100 nM, Bachem, Bubendorf, Switzerland) was bath applied and electrophysiological measurements were repeated 10 min after starting Ucn3 administration. Offline analysis was performed using the Pulse Software and statistical evaluation with SigmaStat 3.5. Statistical comparisons were carried out using two-tailed paired *t*-tests and Wilcoxon two-tailed matched-pairs signed rank tests, with significance declared at $P < 0.05$.

***In vitro* evaluation of optogenetic stimulation protocols.** Acute brain slices from adult (8–10 weeks old) male C57BL/6X129 *Ucn3::Cre* mice bilaterally injected with AAV5-EF1α-DIO-ChR2-eYFP (postnatal days 40–45) were used 3–5 weeks after virus injection as described above. The recording chamber was perfused with carbogenated ACSF at a rate of 2 ml min^{-1} and maintained at 32 °C. Cell attached current clamp recordings or whole-cell patch-clamp recordings were obtained from Ucn3-positive MeA neurons, identified by ChR2-eYFP expression. Patching was performed under visual control using differential interference contrast microscopy (BX51WIF, Olympus) and an Andor Neo sCMOS camera (Andor Technology). Borosilicate glass pipettes (BF100-58-10; Sutter Instrument) were pulled using a laser micropipette puller (P-2000 model, Sutter Instrument, Novato, CA, USA). We pulled glass pipettes with resistances between 4–7 MΩ. The internal solution contained (in mM) 130 potassium gluconate, 10 KCl, 2 $MgCl_2$, 10 HEPES, 10 EGTA (300 mOsm). The pH was adjusted to 7.4 with KOH. For voltage-clamp experiments, neurons were clamped at −70 mV. Optical activation of ChR2-expressing neurons was performed with 475/28 nm light pulses (Lumencor Spectra X; Lumencor) delivered through the microscope illumination path. Recordings were performed with a MultiClamp 700B amplifier, filtered at 8 kHz and digitized at 20 kHz using a Digidata 1440A digitizer (Molecular Devices). Stability of optogenetic $Ucn3^+$ neuron activation was determined by a repeated measures ANOVA on the average number of evoked spikes per stimulation, calculated in 10-s bins (50 stimulations).

Group behavior experiment. Mice were studied in a specialized arena designed for automated tracking of individual and group behavior[17]. Each arena housed a group of four male mice at the age of 12 weeks. The arena consisted of an open 70 × 50 × 50 cm box and included the following objects: Z-shaped wall, a water dispenser, two feeders, a small nest, large nest, an elevated block, and two elevated ramps. Food and water were given *ad libitum*. During the light phase (12 h) arenas were illuminated with 200 lx and during the dark phase (12 h) a 2 lx diffused light provided by two True Light bulbs turned to the ceiling of the room. The mice were recorded in the dark phase using a color-sensitive camera (Panasonic Color CCTV, WV-CL924AE), which was placed 1 m above the arena. The camera analog input is converted to digital information with a digitizer (Picolo Diligent frame grabber board) and recoded on a standard computer. Mouse trajectories were automatically detected offline using custom software in Matlab (MathWorks, Natick, MA, USA).

We subchronically decreased excitability of MeA Ucn3 cells using DREADDs (designer receptors exclusively activated by designer drugs), which are engineered GPCRs (we used $G_{i/o}$-coupled human muscarinic M4 (hM4D)). DREADDs can be selectively activated by the otherwise inactive clozapine analog clozapine-*N*-oxide (CNO).

Functional validation. Ten $Ucn3::Cre^+$ mice (9 weeks old) were injected in the MeA with the conditional hM4D-DREAD expressing virus (AAV8-syn-DIO-hM4D-mCherry). Twenty days later, all animals underwent social defeat during a 5-min encounter with an aggressive ICR mouse. Forty minutes before a social defeat, 5 animals received IP injection of CNO (5 µg per g body weight); the other 5 animals received a saline injection (control). After the 5-min attack period, a perforated clear acrylic glass divider was placed between the animals for 90 min. Subsequently, animals were perfused. To exclude mice that failed to express hM4D-DREAD in the MeA, we stained MeA sections from each brain for mCherry (we did not detect red fluorescence in unstained sections) with rabbit anti-mCherry 1:200 as the primary antibody (Abcam, cat no. ab183628), followed by Alexa Fluor 594 goat anti-rabbit as secondary antibody (Life Technologies, cat. no. A31632). A second set of brain sections were stained for early immediate gene product cFos (the product of the early immediate gene *Fos*). Rabbit anti-cFos antibody (1:200, Santa Cruz Biotechnology cat no. sc-52) was the primary antibody, followed by Alexa Fluor 594 goat anti-rabbit as secondary antibody (Life Technologies, cat. no. A31632).

Experimental design. CNO can also be delivered in drinking water. We used groups of transgenic $Ucn3::Cre^+$ as treatment and groups of $Ucn3::Cre^-$ as controls and stereotaxic injections of adeno-associated-virus carrying a DIO-hM4D fused to mCherry fluorescent protein (AAV8-syn-DIO-hM4D-mCherry) to express the hM4D specifically in MeA Ucn3 cells. The virus was injected bilaterally when the mice were 9 weeks old. Mice were mildly anesthetized with isoflurane. Their eyes were protected against drying using eye gel (Viscotears liquid gel; Alcon).

At the age of 11 weeks, the fur of the mice was stained using a brush with semi-permanent hair dyes. The fur was dried with a fan (low power and heat) for 3 min. After awakening, mice were kept in separate carton boxes for 4 h before reunion. Mice were introduced to the arena for tracking 5 d after the fur staining. The dyes used—namely, Electric Banana (HCR 11012), Pillarbox Red (HCR 11020), and Raven (HCR 11007), from Tish & Snooky's NYC Inc., New York—were composed of natural ingredients. Mice were identified and tracked automatically according to their fur colors, which were learned from labeled data. In the experiment we tested 5 treatment Cre^+ groups with a total of 20 mice, and 3 control Cre^- groups with 12 mice.

Identification and classification of contacts between mice. We automatically identified and classified "contacts" between mice as events in which the distance between two mice (d) was less than 10 cm. We then used the movement direction of one mouse relative to another mouse (θ) to identify the nature of the contact for each of the mice (**Supplementary Fig. 10d**). If, for mouse A, the projection of the direction of its movement relative to mouse B was small enough

$$\left|\tan(\theta)\cdot 2d\right| < \Theta_1, \text{ for } -\frac{\pi}{2} < \theta < \frac{\pi}{2}$$

then it was moving toward B; if

$$\left|\tan(\theta)\cdot 2d\right| < \Theta_2, \text{ for } \frac{\pi}{2} < \theta < \frac{3}{2}\pi$$

it was moving away from it; otherwise it was idle with respect to the other mouse (Θ_1 and Θ_2 were found by optimization).

To classify aggressive and nonaggressive contacts, we first used a hidden Markov model[42] to identify post-contact behaviors in which mouse A was moving toward B and B was moving away from A (**Supplementary Fig. 10e**). We then used 500 manually labeled events to learn statistical classifiers of aggressive and nonaggressive post-contact behavior. For each event we estimated a range of parameters, including individual and relative speed and distance, and optimized a quadratic discriminant classifier[43], a *k*-nearest neighbor algorithm based on these parameters, and a decision-tree classifier that used these parameters at each tree intersection[44]. We found that for a test set of 1,000 events, none of these classifiers were accurate enough individually, but that a combined approach in which we labeled an event as aggressive if any of the classifiers labeled it as such gave ~80% detection with 0.5% false alarms.

Social hierarchy. To describe the dominance hierarchy among the mice, we estimated the relative aggressiveness of each pair, by comparing the number of times mouse *i* chased *j* vs. the other way around. If this number was significantly higher for one than the other, then this mouse was ranked higher (as more dominant) than the other (significance was determined using the Clopper-Pearson test[45]). Next the hierarchy map was set as the lowest tree to preserve these ranks, using algorithm similar to the topological sorting algorithm[46] but extended to allow two or more mice to occupy the same rank.

We used the normalized David's score to assign each individual a continuous measure of its social rank[47]. David's score assumes a linear hierarchy, where each pair from the group contains a dominant and a subordinate individual. It is estimated by using the fraction of the interactions P_{ij} in which mouse *i* chased mouse *j* relative to the total number of agonistic interactions. David's score of each individual is then computed as the sum

$$\mathrm{DS}_i = w^i + w_2^i - l^i - l_2^i$$

where

$$w^i = \sum_{j \neq i} P_{ij}$$

is the sum of the fraction of times that mouse *i* has 'won' (i.e., was the chaser) and

$$w_2^i = \sum_{j \neq i} w^j P_{ij}$$

is a similar sum weighted by the w^j of the other mice, while

$$l^i = \sum_{j \neq i} P_{ji}$$

is the sum of the fractions of 'losses' (escapes), and accordingly

$$l_2^i = \sum_{j \neq i} w^j P_{ji}$$

is its weighted sum. The score is then normalized to the range between 0 and $N - 1$ (where N is the number of subjects; $N = 4$ in our tests) by using the following formula:

$$\mathrm{NormDS} = \frac{1}{N}\left(\mathrm{DS} + \frac{N(N-1)}{2}\right)$$

Statistical analyses. *Social approach test.* The time the treated mice spent in each chamber, relative to the average time of the control mice, was analyzed by repeated-measures analysis of variance. Since the time spent in the arena was summed to 30 min, the scores for the three side chambers and the introduction zone are mutually exclusive rather than independent measures. Therefore, statistical comparisons were between the three side chambers without the introduction zone. Differences between control and treated mice in interacting with novel or familiar conspecifics were analyzed by two-tailed Student's *t*-test or in a case of directional prediction by one-tailed Student's *t*-test.

Novel object preference, open field, light/dark transfer. Differences between WT and treated mice and *Crfr2* KO mice were analyzed by two-tailed Student's *t*-test.

General locomotor activity during 3 consecutive days. Differences between WT and *Crfr2* KD mice were analyzed by RM two-way ANOVA.

Quantification of Ucn3 effects on CRF-R2-expressing neurons. Increased depolarization was analyzed by Wilcoxon two-tailed matched-pairs signed rank test, increased input resistance and increased AP firing were analyzed by paired two-tailed *t*-test.

Electrophysiological confirmation of optogenetic activation of MeA Ucn3-ChR2-expressing neurons. Correlation of photocurrents and light power was analyzed by RM-ANOVA.

Chronic social defeat and Shank3 KO mice. MeA mRNA of *Crfr2* was analyzed by two-tailed Mann Whitney test.

Functional validation of DREADD based MeA Ucn3 inhibition. Quantification of cFos staining was analyzed by one-tailed Mann Whitney test. Equal variance was verified between control and treated groups in all experiments. When parametric tests were used, data were tested for normality. Individual mice were excluded from all behavioral analysis if data differed more than 2 s.d. from mean.

In the group behavior experiments, we used a permutation test to determine statistical significance[48]. Since this is a non-parametric approach, there is no need to assume any prior regarding the underlying distribution (such as normality). In a permutation test, we test the null hypothesis that the average change between two conditions A and B is zero. We take the experimental data and randomly permute the labels of the two conditions (preserving the original number of labels for each condition). For each random permutation we then compute the difference in the median between the two conditions. By repeatedly shuffling the labels and measuring the difference in medians, we obtain a distribution that we then compare to the actual difference of the original, unshuffled data. Taking the absolute value of this actual distance, the fraction of randomized trials in which the difference is higher than this value or lower than the negative of this value gives the *P*-value (in a two-tailed test). In none of the experiments in this work were the experimenters blinded to the treatment.

Sample size and randomization of experimental groups. In experiment that involved *Ucn3* KO and *Crfr2* KO mice, mice were obtained from heterozygous parents and kept in mixed cages with their WT siblings. In experiments that involved *Ucn3::Cre* or *Crfr2::Cre* lines, mice were obtained from heterozygous father and WT mother. Heterozygous Cre^+ mice were kept together in mixed cages with their WT siblings. In the *Crfr2* KD experiment, mice were randomly assigned to *Crfr2* KD or control groups. In the pharmacological Ucn3 administration experiment, mice were cannulated and randomly assigned to saline and mUcn3 groups. At the end of the experiment the same animals were reassigned for mUcn3 + saline and mUcn3 + antagonist groups. For all experiments, no statistical methods were used to predetermine sample sizes, but our sample sizes are similar to those generally employed in the field[8].

A **Supplementary Methods Checklist** is available.

Data availability. The data that support the findings of this study are available from the corresponding author upon request.

42. Rabiner, L.R. A tutorial on hidden Markov models and selected applications in speech recognition. *Proc. IEEE* **77**, 257–286 (1989).
43. Duda, R.O., Hart, P.E. & Stork, D.G. *Pattern Classification and Scene Analysis* 2nd ed. (Wiley Interscience, 1995).
44. Breiman, L., Friedman, J., Stone, C.J. & Olshen, R.A. *Classification and Regression Trees* (CRC Press, 1984).
45. Clopper, C.J. & Pearson, E.S. The use of confidence or fiducial limits illustrated in the case of the binomial. *Biometrika* **26**, 404–413 (1934).
46. Cormen, T.H. *Introduction to Algorithms* (MIT Press, 2009).
47. de Vries, H., Stevens, J.M. & Vervaecke, H. Measuring and testing the steepness of dominance hierarchies. *Anim. Behav.* **71**, 585–592 (2006).
48. Howell, D. *Statistical Methods for Psychology* (Cengage Learning, 2012).

doi:10.1038/nn.4346